

Synthesis and Characterization of Heterodinuclear IrCo, RuCo, IrNi, and RuNi Complexes Containing Pyrazolate and Pyrazolylborate Ligands

Daniel Carmona,^{*,†} Fernando J. Lahoz,[†] Reinaldo Atencio,[†] Andrew J. Edwards,[†]
Luis A. Oro,^{*,†} M. Pilar Lamata,[‡] Montserrat Esteban,[‡] and Swiatoslaw Trofimenko^{*,§}

Departamento de Química Inorgánica, Facultad de Ciencias, Instituto de Ciencia de Materiales de Aragón, Universidad de Zaragoza-Consejo Superior de Investigaciones Científicas, 50009 Zaragoza, Spain, Departamento de Química Inorgánica, Escuela Universitaria de Ingeniería Técnica e Industrial, Instituto de Ciencia de Materiales de Aragón, Universidad de Zaragoza, Corona de Aragón 35, 50009 Zaragoza, Spain, and Du Pont Central Research and Development, Experimental Station, Wilmington, Delaware 19880-0302

Received July 14, 1995[⊗]

Treatment of the metallo ligands [ML(pz)₂(Hpz)] (pz = pyrazolate; L = C₅Me₅, M = Ir (**1**); L = mesitylene, M = Ru (**3**)) with [M'Cl{HB(3-*i*-Pr-4-Br-pz)₃}] (M' = Co (**4**), Ni (**5**)) yields heterodinuclear complexes of formula [LM(μ-pz)₂(μ-Cl)M'{HB(3-*i*-Pr-4-Br-pz)₃}] (L = C₅Me₅; M = Ir; M' = Co (**6**), Ni (**7**)). L = mesitylene; M = Ru; M' = Co (**8**)). The related complex [Ru(η⁶-*p*-cymene)(pz)₂(Hpz)] (**2**) reacts with equimolar amounts of **4** or **5** to give mixtures of the corresponding bis(μ-pyrazolato) μ-chloro complexes [(η⁶-*p*-cymene)Ru(μ-pz)₂(μ-Cl)-M'{HB(3-*i*-Pr-4-Br-pz)₃}] (M' = Co (**9**), Ni (**10**)) and the triply pyrazolato-bridged complexes [(η⁶-*p*-cymene)-Ru(μ-pz)₃M'{HB(3-*i*-Pr-4-Br-pz)₃}] (M' = Co (**11**), Ni (**12**)). Complex **1** reacts with **5** in the presence of KOH to give the IrNi complex [(η⁵-C₅Me₅)Ir(μ-pz)₃Ni{HB(3-*i*-Pr-4-Br-pz)₃}] (**13**) whereas its reaction with **4** and KOH rendered the bis(μ-pyrazolato) μ-hydroxo complex [(η⁵-C₅Me₅)Ir(μ-pz)₂(μ-OH)Co{HB(3-*i*-Pr-4-Br-pz)₃}] (**14**). The molecular structure of the heterobridged IrCo complex (**6**) and those of the homobridged RuNi (**12**) and IrNi (**13**) complexes have been determined by X-ray analyses. Compound **6** crystallizes in the monoclinic space group *P*2₁/*n*, with *a* = 10.146(5) Å, *b* = 18.435(4) Å, *c* = 22.187(13) Å, β = 97.28(4)°, and *Z* = 4. Complex **12** is monoclinic, space group *P*2₁, with *a* = 10.1169(7) Å, *b* = 21.692(2) Å, *c* = 11.419(1) Å, β = 112.179(7)°, and *Z* = 2. Compound **13** crystallizes in the monoclinic space group *Cc*, with *a* = 13.695(2) Å, *b* = 27.929(6) Å, *c* = 13.329(2) Å, β = 94.11(4)°, and *Z* = 4. All the neutral complexes **6**, **12**, and **13** consist of linear M···M'···B backbones with two (**6**) or three (**12**, **13**) pyrazolate ligands bridging the dimetallic M···M' units and three substituted 3-*i*-Pr-4-Br-pz groups joining M' to the boron atoms. The presence in the proximity of the first-row metal M' of the three space-demanding isopropyl substituents of the pyrazolate groups induces a significant trigonal distortion of the octahedral symmetry, yielding clearly different M'–N bond distances on both sides of the ideal octahedral coordination sphere of these metals.

Introduction

An extensive coordination chemistry has been developed from poly(pyrazolylborate) anions which includes most transition-metal ions.¹ In particular, the complexes² [M'Cl{HB(3-*i*-Pr-4-Br-pz)₃}] (M' = Co, Ni), due to the presence of this particular tris(pyrazolyl)borate ligand, possess a favorable combination of steric protection around the metal and selective accessibility toward other ligands that make them very suitable for controlled preparation of mixed species [LM'{HB(3-*i*-Pr-4-Br-pz)₃}]. These mixed complexes are five- or six-coordinate depending on the coordination capacity of L. Thus, for example, when L is HB(pz)₃, the heteroleptic [{HB(pz)₃}M'{HB(3-*i*-Pr-4-Br-pz)₃}] C_{3v} octahedral complexes are obtained,^{1d,3} whereas when L is acetylacetonate, tropolonate, or dithiocarbamate, the corresponding [LM'{HB(3-*i*-Pr-4-Br-pz)₃}] compounds possess five-coordinate geometry.^{1d,3}

From a coordination point of view, the complexes [Ir(η⁵-C₅-Me₅)(pz)₂(Hpz)],⁴ [Ru(η⁶-*p*-cymene)(pz)₂(Hpz)],⁵ and [Ru(η⁶-mesitylene)(pz)₂(Hpz)] are comparable to protonated tris(pyrazolyl)borates or to the Kläui ligands, such as [(η⁵-C₅H₅)Co{PO(OR)₂}₃].⁶ In fact, we have shown that the iridium^{7,8} and the ruthenium⁹ anions [Ir(η⁵-C₅Me₅)(pz)₃][−] and [Ru(η⁶-*p*-cymene)(pz)₃][−] represent a new class of tripodal mononegative ligands, capable of coordinating via either two^{7,9} or three⁸ pz links. In order to explore the coordination capacity of these compounds as tridentate ligands, we have attempted the preparation of heterodinuclear MM' species by reacting them with poly(pyrazolyl)borato complexes [M'Cl{HB(3-*i*-Pr-4-Br-pz)₃}] (M' = Co, Ni).

- (3) Calabrese, J. C.; Domaille, P. J.; Thompson, J. S.; Trofimenko, S. *Inorg. Chem.* **1990**, *29*, 4429.
- (4) Carmona, D.; Oro, L. A.; Lamata, M. P.; Elguero, J.; Apreda, M. C.; Foces-Foces, C.; Cano, F. H. *Angew. Chem., Int. Ed. Engl.* **1986**, *25*, 1114.
- (5) Carmona, D.; Ferrer, J.; Oro, L. A.; Agreda, M. C.; Foces-Foces, C.; Cano, F. H. *J. Chem. Soc., Dalton Trans.* **1990**, 1463.
- (6) Kläui, W. *Angew. Chem., Int. Ed. Engl.* **1990**, *29*, 627.
- (7) Carmona, D.; Lahoz, F. J.; Oro, L. A.; Lamata, M. P.; Buzarra, S. *Organometallics* **1991**, *10*, 3123.
- (8) Carmona, D.; Lamata, M. P.; Ferrer, J.; Modrego, J.; Perales, M.; Lahoz, F. J.; Atencio, R.; Oro, L. A. *J. Chem. Soc., Chem. Commun.* **1994**, 575.
- (9) Carmona, D.; Ferrer, J.; Lahoz, F. J.; Atencio, R.; Oro, L. A.; Lamata, M. P. *Organometallics* **1995**, *14*, 2057.

[†] Facultad de Ciencias, Universidad de Zaragoza.

[‡] EUTI, Universidad de Zaragoza.

[§] Du Pont.

[⊗] Abstract published in *Advance ACS Abstracts*, March 15, 1996.

- (1) (a) Trofimenko, S. *Acc. Chem. Res.* **1971**, *4*, 17. (b) Trofimenko, S. *Chem. Rev.* **1972**, *72*, 497. (c) Trofimenko, S. *Prog. Inorg. Chem.* **1986**, *34*, 115. (d) Trofimenko, S. *Chem. Rev.* **1993**, *93*, 943.
- (2) Trofimenko, S.; Calabrese, J. C.; Domaille, P. J.; Thompson, J. S. *Inorg. Chem.* **1989**, *28*, 1091.

Here we report the preparation of new heterodinuclear MM' complexes with pyrazolate and other mononegative bridging ligands such as chloride or hydroxide anions starting from [ML-(pz)₂(Hpz)] (ML = Ir(η^5 -C₅Me₅), Ru(η^6 -*p*-cymene), Ru(η^6 -mesitylene), and [M'Cl{HB(3-*i*-Pr-4-Br-pz)₃}] (M' = Co, Ni) complexes. The molecular structures of the complexes [(η^5 -C₅Me₅)Ir(μ -pz)₂(μ -Cl)Co{HB(3-*i*-Pr-4-Br-pz)₃}] (**6**), [η^6 -*p*-cymene)Ru(μ -pz)₃Ni{HB(3-*i*-Pr-4-Br-pz)₃}] (**12**) and [(η^5 -C₅Me₅)Ir(μ -pz)₃Ni{HB(3-*i*-Pr-4-Br-pz)₃}] (**13**) are also reported.

Experimental Section

The complexes [Ir(η^5 -C₅Me₅)(pz)₂(Hpz)]₂,⁴ [Ru(η^6 -*p*-cymene)(pz)₂(Hpz)]₂,⁵ and [M'Cl{HB(3-*i*-Pr-4-Br-pz)₃}]₂ (M' = Co, Ni) were prepared by literature procedures. [Ir(η^5 -C₅Me₅)Cl(Hpz)₂]BF₄,¹⁰ [Ru(η^6 -mesitylene)(pz)₂(Hpz)]₂,¹¹ and [Ru(η^6 -mesitylene)(Hpz)₃][BF₄]₂¹² were prepared as described for the related [Rh(η^5 -C₅Me₅)Cl(Hpz)₂]-BF₄,¹³ [Ru(η^6 -*p*-cymene)(pz)₂(Hpz)]₂⁵ and [Ru(η^6 -*p*-cymene)(Hpz)₃]-[BF₄]₂,⁵ respectively. All solvents were dried over appropriate drying agents, distilled under N₂, and degassed prior to use. All preparations were carried out under nitrogen. Infrared spectra were obtained as Nujol mulls with a Perkin-Elmer 1330 spectrophotometer. The C, H, and N analyses were carried out with a Perkin-Elmer 240 B microanalyzer. ¹H NMR spectra were recorded on a Varian UNITY 300 spectrometer. Paramagnetic compounds were studied with a sweep width of 90 kHz and 45° pulse angles. FAB⁺ MS spectra were recorded on a VG Autospec spectrometer. The EPR spectra were measured either at room temperature or at liquid-nitrogen temperature. Powdered polycrystalline samples were introduced into a quartz tube. The spectra were recorded using a Bruker ESP380E spectrometer working in X-band. Magnetic measurements were made using a commercial SQUID magnetometer from Quantum Design. Susceptibility measurements were carried out at a field of 1 T produced by a superconducting coil. Additional magnetization measurements were made up to 5 T at 1.8 and 3.0 K.

Synthesis of [(η^5 -C₅Me₅)Ir(μ -pz)₂(μ -Cl)M'{HB(3-*i*-Pr-4-Br-pz)₃}] (M' = Co (6**), Ni (**7**)).** A mixture of [Ir(η^5 -C₅Me₅)(pz)₂(Hpz)] (120.0 mg, 0.226 mmol) and [M'Cl{HB(3-*i*-Pr-4-Br-pz)₃}] (0.226 mmol) in methanol (20 mL) was stirred for 2 h. The orange-yellow **6** or yellow **7** precipitate was filtered off, washed with methanol, and dried under vacuum. Recrystallization from chloroform–hexane led to orange (**6**) or yellow (**7**) crystals.

6: yield 250.0 mg, 78%. ¹H NMR in CDCl₃ (ppm, relative ratios, assignments): 90.0, 89.2, 82.2, 71.6, 51.7, 14.6, -16.5, -37.2, -38.1, -80.2, -90.8, -131.8; 1:2:2:1:2:15:6:6:2:2:1; BH, 5-H of (pz)₂ nearest to Ir, 5-H of (3-*i*-Pr-4-Br-pz)₂ *cis* to Cl, 5-H of 3-*i*-Pr-4-Br-pz *trans* to Cl, 4-H of (pz)₂, C₅Me₅, CHMe₂ *trans* to Cl, CHMeMe *cis* to Cl inner position, CHMeMe *cis* to Cl outer position, 3-H of (pz)₂ nearest to Co, CHMe₂ *cis* to Cl, CHMe₂ *trans* to Cl. IR (cm⁻¹): ν (BH) 2440. FAB⁺ MS (*m/z*): 1131. Anal. Calcd for C₃₄H₄₆BBR₃ClCoIrN₁₀: C, 36.08; H, 4.10; N, 12.37. Found: C, 35.73; H, 3.92; N, 12.37.

7: yield 256.1 mg, 80%. IR (cm⁻¹): ν (BH) 2440. FAB⁺ MS (*m/z*): 1132. Anal. Calcd for C₃₄H₄₆BBR₃ClIrN₁₀Ni: C, 36.09; H, 4.10; N, 12.38. Found: C, 36.35; H, 3.97; N, 12.51.

Alternatively, complex **6** could be prepared by treating [Ir(η^5 -C₅Me₅)Cl(Hpz)₂]BF₄ (100.0 mg, 0.171 mmol) and [CoCl{HB(3-*i*-Pr-4-Br-pz)₃}] (114.0 mg, 0.171 mmol) with a methanolic solution of KOH (2.59 mL, 0.132 mol L⁻¹, 0.342 mmol) in methanol (20 mL). The mixture was stirred for 2 h, and the solid which precipitated spontane-

ously was filtered off, washed with water and methanol, and vacuum-dried (155.1 mg, 80% yield).

Synthesis of [(η^6 -mesitylene)Ru(μ -pz)₂(μ -Cl)Co{HB(3-*i*-Pr-4-Br-pz)₃}] (8**).** To a solution of [Ru(η^6 -mesitylene)(pz)₂(Hpz)] (130.0 mg, 0.307 mmol) in acetone (20 mL) were added NEt₃ (42.6 μ L, 0.307 mmol) and [CoCl{HB(3-*i*-Pr-4-Br-pz)₃}] (205.8 mg, 0.307 mmol). After 16 h of stirring, precipitation of an orange solid was observed, which was filtered off, washed with acetone and water, and dried under vacuum (189.2 mg, 60% yield). Recrystallization from chloroform–hexane led to red crystals. ¹H NMR in CDCl₃ (ppm, relative ratios, assignments): 90.6, 86.7, 81.9, 68.7, 53.9, 28.7, 12.6, -15.9, -36.9, -37.3, -77.0, -92.0, -125.0; 2:1:2:1:2:3:9:6:6:6:2:2:1; 5-H of (pz)₂ nearest to Ru, BH, 5-H of (3-*i*-Pr-4-Br-pz)₂ *cis* to Cl, 5-H of 3-*i*-Pr-4-Br-pz *trans* to Cl, 4-H of (pz)₂, C₆H₃Me₃, C₆H₃Me₃, CHMe₂ *trans* to Cl, CHMeMe *cis* to Cl inner position, CHMeMe *cis* to Cl outer position, 3-H of (pz)₂ nearest to Co, CHMe₂ *cis* to Cl, CHMe₂ *trans* to Cl. IR (cm⁻¹): ν (BH) 2450. FAB⁺ MS (*m/z*): 1027. Anal. Calcd for C₃₃H₄₃BBR₃ClCoN₁₀Ru: C, 38.64; H, 4.23; N, 13.65. Found: C, 38.84; H, 4.09; N, 13.59.

Reaction of [Ru(η^6 -*p*-cymene)(pz)₂(Hpz)] with [M'Cl{HB(3-*i*-Pr-4-Br-pz)₃}] (M' = Co, Ni). A solution of [Ru(η^6 -*p*-cymene)(pz)₂(Hpz)] (110.0 mg, 0.251 mmol) and [M'Cl{HB(3-*i*-Pr-4-Br-pz)₃}] (0.251 mmol) in methanol (20 mL) was stirred for 2 h. A mixture of **9** and **11** (145.3 mg) or **10** and **12** (150.5 mg) precipitated, which was filtered off, washed with methanol, and dried under vacuum.

9: ¹H NMR in CDCl₃ (ppm, relative ratios, assignments) 8.2, -16.4, -38.1, -38.5; 6:6:6:6; CHMe₂ (*p*-cymene), CHMe₂ *trans* to Cl, CHMeMe *cis* to Cl inner position, CHMeMe *cis* to Cl outer position. FAB⁺ MS (*m/z*): 1039.

10: FAB⁺ MS (*m/z*) 1040.

Synthesis of [(η^6 -*p*-cymene)Ru(μ -pz)₃M'{HB(3-*i*-Pr-4-Br-pz)₃}] (M' = Co (11**), Ni (**12**)).** A mixture of [Ru(η^6 -*p*-cymene)(pz)₂(Hpz)] (65.3 mg, 0.149 mmol) in methanol (20 mL), NEt₃ (20.7 μ L, 0.149 mmol), and [M'Cl{HB(3-*i*-Pr-4-Br-pz)₃}] (0.149 mmol) was stirred for 2 h. The yellow complex which precipitated spontaneously was filtered off, washed with water and hexane, and vacuum-dried. Recrystallization of complex **12** from dichloromethane–hexane led to yellow crystals.

11: yield 120.2 mg, 75%. ¹H NMR in CD₂Cl₂ (ppm, relative ratios, assignments): 113, 94.3, 90.3, 43.0, 42.3, 36.8, 27.3, 26.2, 17.1, -36.2, -128, -137; 1:3:3:2:2:3:1:3:6:18:3:3; BH, 5-H of (pz)₃ nearest to Ru, 5-H of (3-*i*-Pr-4-Br-pz)₃, C₆H₂H₂, C₆H₂H₂, 4-H of (pz)₃, CHMe₂ (*p*-cymene), CH₃ (*p*-cymene), CHMe₂ (*p*-cymene), CHMe₂ ((3-*i*-Pr-4-Br-pz)₃), 3-H of (pz)₃ nearest to Co, CHMe₂ ((3-*i*-Pr-4-Br-pz)₃). IR (cm⁻¹): ν (BH) 2440. FAB⁺ MS (*m/z*): 1072. Anal. Calcd for C₃₇H₄₈BBR₃CoN₁₂Ru: C, 41.48; H, 4.52; N, 15.69. Found: C, 41.35; H, 4.54; N, 15.50.

12: yield 114.4 mg, 72%. IR (cm⁻¹): ν (BH) 2440. FAB⁺ MS (*m/z*): 1073. Anal. Calcd for C₃₇H₄₈BBR₃N₁₂NiRu: C, 41.49; H, 4.52; N, 15.69. Found: C, 41.80; H, 4.64; N, 15.29.

Synthesis of [(η^5 -C₅Me₅)Ir(μ -pz)₃Ni{HB(3-*i*-Pr-4-Br-pz)₃}] (13**).** A mixture of [Ir(η^5 -C₅Me₅)(pz)₂(Hpz)] (118.3 mg, 0.223 mmol), KOH (0.705 mL, 0.316 mol L⁻¹, 0.223 mmol), and [NiCl{HB(3-*i*-Pr-4-Br-pz)₃}] (149.4 mg, 0.223 mmol) in methanol (20 mL) was stirred for 2 h. A green-yellow solid precipitated which was filtered off, washed with methanol, and dried under vacuum (189.7 mg, 73% yield). Recrystallization from chloroform–hexane led to green-yellow crystals. IR (cm⁻¹): ν (BH) 2440. Anal. Calcd for C₃₇H₄₉BBR₃IrN₁₂Ni: C, 38.20; H, 4.25; N, 14.45. Found: C, 38.18; H, 4.32; N, 14.19.

Synthesis of [(η^5 -C₅Me₅)Ir(μ -pz)₂(μ -OH)Co{HB(3-*i*-Pr-4-Br-pz)₃}] (14**).** A mixture of [Ir(η^5 -C₅Me₅)(pz)₂(Hpz)] (118.3 mg, 0.223 mmol), KOH (1.409 mL, 0.316 mol L⁻¹, 0.446 mmol), and [CoCl{HB(3-*i*-Pr-4-Br-pz)₃}] (150.0 mg, 0.223 mmol) in methanol (20 mL) was stirred for 3 h. The resulting brown solid (116.5 mg), a mixture of **14** (94%) and **6** (6%), was filtered off, washed with methanol, and vacuum-dried. ¹H NMR in CDCl₃ (ppm, relative ratios, assignments): 111, 94.9, 86.4, 85.6, 47.3, 27.4, 23.6, -32.6, -33.9, -41.1, -99, -123, -134; 1:2:2:1:2:1:15:6:6:6:2:1:2; BH, 5-H of (pz)₂ nearest to Ir, 5-H of (3-*i*-Pr-4-Br-pz)₂ *cis* to OH, 5-H of 3-*i*-Pr-4-Br-pz *trans* to OH, 4-H of (pz)₂, OH, C₅Me₅, CHMeMe *cis* to OH inner position, CHMeMe *cis* to OH outer position, CHMe₂ *trans* to OH, 3-H of (pz)₂

(10) [Ir(η^5 -C₅Me₅)Cl(Hpz)₂]BF₄: 85% yield. ¹H NMR (ppm, CDCl₃): 11.9 (br s, 2H, NH), 8.02 (br d, *J* = 1.7 Hz, 2H, 3-H of (pz)₂), 7.67 (d, *J* = 2.7 Hz, 2H, 5-H of (pz)₂), 6.47 (t, *J* = 2.4 Hz, 2H, 4-H of (pz)₂), 1.58 (s, 15H, C₅Me₅). IR (cm⁻¹): ν (NH) 3280.

(11) [Ru(η^6 -mesitylene)(pz)₂(Hpz)]₂: 82% yield. ¹H NMR (ppm, CDCl₃): 12.43 (br s, 1H, NH), 7.65 (d, *J* = 1.7 Hz, 3H, 3-H of (pz)₃), 6.94 (br s, 3H, 5-H of (pz)₃), 6.12 (t, *J* = 1.83 Hz, 3H, 4-H of (pz)₃), 5.04 (s, 3H, C₆H₃Me₃), 1.76 (s, 9H, C₆H₃Me₃). IR (cm⁻¹): ν (NH) 3200–2000 vbr.

(12) [Ru(η^6 -mesitylene)(Hpz)₃][BF₄]₂: 85% yield. ¹H NMR (ppm, (CD₃)₂CO): 12.7 (br s, 3H, NH), 8.20 (br s, 3H, 3-H of (pz)₃), 7.22 (br s, 3H, 5-H of (pz)₃), 6.67 (br s, 3H, 4-H of (pz)₃), 6.09 (s, 3H, C₆H₃Me₃), 1.99 (s, 9H, C₆H₃Me₃). IR (cm⁻¹): ν (NH) 3160, 3320.

(13) Carmona, D.; Oro, L. A.; Lamata, M. P.; Puebla, M. P.; Ruiz, J.; Maitlis, P. M. *J. Chem. Soc., Dalton Trans.* **1987**, 639.

Table 1. Summary of Crystallographic Data for Complexes **6**, **12**·CH₂Cl₂, and **13**·2CHCl₃

	6 (Ir/Co)	12 (Ru/Ni)	13 (Ir/Ni)
formula	C ₃₄ H ₄₆ BBr ₃ ClCoIrN ₁₀	C ₃₇ H ₄₈ BBr ₃ N ₁₂ NiRu·CH ₂ Cl ₂	C ₃₇ H ₄₉ BBr ₃ IrN ₁₂ Ni·2CHCl ₃
mol wt	1151.93	1156.12	1402.07
<i>a</i> , Å	10.146(5)	10.1169(7)	13.695(2)
<i>b</i> , Å	18.435(4)	21.692(2)	27.929(6)
<i>c</i> , Å	22.187(13)	11.419(1)	13.329(2)
β , deg	97.28(4)	112.179(7)	94.11(4)
<i>V</i> , Å ³	4116(3)	2320.6(6)	5085(2)
cryst syst	monoclinic	monoclinic	monoclinic
space group	<i>P</i> 2 ₁ / <i>n</i>	<i>P</i> 2 ₁	<i>Cc</i>
<i>Z</i>	4	2	4
temp, °C	-100	-50	-100
scan method	ω -2 θ	ω -2 θ	ω -2 θ
θ min-max, deg	2-25	2-25	2-25
octants	- <i>h</i> , - <i>k</i> , \pm <i>l</i>	- <i>h</i> , \pm <i>k</i> , \pm <i>l</i>	- <i>h</i> , <i>k</i> , \pm <i>l</i>
no. of measd refls	7668	9189	10528
no. of indep refls	7136	8212	8959
no. of params	475	536	583
GOF	1.032	1.017	1.048
ρ_{calcd} , g cm ⁻³	1.826	1.652	1.831
μ , mm ⁻¹	6.65	3.47	4.127
<i>F</i> (000)	2204	1156	2484
transm coeff	0.017-0.042	0.299-0.596	0.223-0.454
<i>R</i> (int)	0.0385	0.0181	0.0202
<i>R</i> ₁ ^a	0.0480	0.0278	0.0352
<i>R</i> ₂ ^a (all data)	0.1257	0.0655	0.0882

^a SHELXL-93:¹⁶ $R_1 = \sum |F_o| - |F_c| / \sum |F_o|$ calculated using 4894, 7754, and 8429 observed reflections [$F_o > 4\sigma(F_o)$] for complexes **6**, **12**, and **13**, respectively. $R_2 = [\sum w(F_o^2 - F_c^2)^2 / \sum wF_o^4]^{1/2}$, with $w^{-1} = [\sigma^2(F_o^2) + (xP)^2 + yP]$ and $P = F_o^2 + 2F_c^2/3$.

nearest to Co, CHMe₂ *trans* to OH, CHMe₂ *cis* to OH. IR (cm⁻¹): ν (BH) 2440, ν (OH) 3640. FAB⁺ MS (*m/z*): 1113.

X-ray Structure Analyses of [(η^5 -C₅Me₅)Ir(μ -pz)₂(μ -Cl)Co{HB(3-*i*-Pr-4-Br-pz)₃}] (6**), [(η^6 -*p*-cymene)Ru(μ -pz)₃Ni{HB(3-*i*-Pr-4-Br-pz)₃}]·CH₂Cl₂ (**12**·CH₂Cl₂), and [(η^5 -C₅Me₅)Ir(μ -pz)₂Ni{HB(3-*i*-Pr-4-Br-pz)₃}]·2CHCl₃ (**13**·2CHCl₃).** A summary of crystal data and refinement parameters is reported in Table 1. Atomic coordinates are listed in Tables 2-4. In the case of complexes **6** and **13**, an oil-coated rapidly cooled crystal of suitable size was mounted onto a glass fiber directly from solution;¹⁴ for complex **12**, the selected crystal was glued onto the tip of a glass fiber. A set of randomly searched reflections were indexed to the corresponding crystal symmetry and accurate unit cell dimensions determined by least-squares refinement of 24 carefully centered reflections ($25 \leq 2\theta \leq 30^\circ$). Data were collected on a Stoe AED diffractometer, with graphite-monochromated Mo K α radiation ($\lambda = 0.71073$ Å) by the $\omega/2\theta$ scan method. Three orientation and intensity standards were monitored every 55 min of measuring time throughout data collection; no variation was observed. All data were corrected for absorption using an empirical method (ψ scan) applied using the program XEMP;¹⁵ minimum and maximum transmission factors are listed in Table 1. All structures were solved by direct methods (SHELXTL PLUS)¹⁵ and conventional Fourier techniques. For the three structures, all non-hydrogen atoms were refined anisotropically and the hydrogen atom bonded to the boron was located and freely refined as an isotropic atom. Remaining hydrogens were included in fixed idealized positions. The function minimized was $\sum [w(F_o^2 - F_c^2)^2]$ with the weight defined as $w^{-1} = [\sigma^2(F_o^2) + (xP)^2 + yP]$ ($P = F_o^2 + 2F_c^2/3$). Atomic scattering factors, corrected for anomalous dispersion for metal, Br, and Cl atoms, were used as implemented in the refinement programs.¹⁶

Data for 6. Crystals suitable for the X-ray diffraction study were obtained from a hexane/chloroform solution. A red crystalline rectangular block of approximate dimensions 0.38 × 0.23 × 0.19 mm was indexed to monoclinic symmetry. The structure was refined by full-matrix least-squares on *F*² (SHELXL-93)¹⁶ to $R_1 = 0.0480$ [$F_o > 4\sigma(F_o)$, for 4894 reflections] and $R_2 = 0.1257$ (all data), with weighting parameters $x = 0.0536$ and $y = 25.8266$ (see Table 1). Largest peak and hole in the final difference map were 1.41 and -0.97 e Å⁻³.

Data for 12. Suitable crystals were obtained from a dichloromethane/hexane solution. A yellow prismatic block of approximate dimensions 0.68 × 0.38 × 0.16 mm was used in the analysis. The structure was refined by full-matrix least-squares on *F*² (SHELXL-93)¹⁶ to $R_1 = 0.0278$ [$F_o > 4\sigma(F_o)$, for 7754 reflections] and $R_2 = 0.0655$, with weighting parameters $x = 0.0302$ and $y = 2.2547$. A solvent molecule of dichloromethane was located in the asymmetric unit. The Flack absolute structure parameter was included in the last stages of the refinement and converged to 0.001(5).¹⁷ Largest peak and hole in the final difference map were 0.59 and -0.57 e Å⁻³.

Data for 13. Crystals suitable for the X-ray diffraction study were obtained from a hexane/chloroform solution. A green-yellow crystalline rectangular block of approximate dimensions 0.44 × 0.37 × 0.10 mm was mounted and indexed to monoclinic symmetry. The structure was refined by full-matrix least-squares on *F*² (SHELXL-93)¹⁶ to $R_1 = 0.0352$ [$F_o > 4\sigma(F_o)$, for 8429 reflections] and $R_2 = 0.0882$ (with $x = 0.067$ and $y = 7.6533$; see Table 1). Two solvent molecules of chloroform were located in the asymmetric unit. The Flack parameter refined to -0.035(6) as an indication of a correct determination of the absolute structure.¹⁷ Residuals peaks in the final difference map were 0.91 and -0.80 e Å⁻³.

Results and Discussion

Chart 1 summarizes all the reactions reported below.

The reaction of the metallo-ligand complexes [ML(pz)₂(Hpz)] (ML = Ir(η^5 -C₅Me₅) (**1**), Ru(η^6 -mesitylene) (**3**)) with the halide compounds [M'Cl{HB(3-*i*-Pr-4-Br-pz)₃}] (M' = Co (**4**), Ni (**5**)) proceeded with displacement of one molecule of pyrazole and afforded the dinuclear complexes [LM(μ -pz)₂(μ -Cl)M'{HB(3-*i*-Pr-4-Br-pz)₃}] (LM = (η^5 -C₅Me₅)Ir; M' = Co (**6**), Ni (**7**)). LM = (η^6 -mesitylene)Ru; M' = Co (**8**)). The yield of **8** was increased from 33 to 60% by adding 1 equiv of NEt₃ to the reaction medium. The IR spectra showed the expected BH stretching at *ca.* 2440 cm⁻¹. In all cases, the ¹H NMR spectra spanned 200-250 ppm, as expected for paramagnetic molecules. For all nickel-containing compounds reported in this paper, the ¹H NMR spectra consisted of very broad unresolved signals, and consequently, no additional information was obtained from

(14) Kottke, T.; Stalke, D. *J. Appl. Crystallogr.* **1993**, *26*, 615.

(15) Sheldrick, G. M. *SHELXTL PLUS*; Siemens Analytical X-ray Instruments, Inc.: Madison, WI, 1990.

(16) Sheldrick, G. M. *SHELXL-93: Program for crystal structure refinement*; University of Göttingen: Göttingen, Germany, 1993.

(17) (a) Flack, H. D. *Acta Crystallogr.* **1983**, *A39*, 876. (b) Glazer, A. M. *Acta Crystallogr.* **1989**, *A45*, 234.

Table 2. Final Atomic Coordinates ($\times 10^4$; $\times 10^5$ for Ir, Co, and Br Atoms) and Equivalent Isotropic Displacement Parameters ($\text{\AA}^2 \times 10^3$) for **6**

atom	x	y	z	$U(\text{eq})^a$
Ir	19801(4)	26447(2)	7953(2)	30(1)
Co	-4334(11)	22695(7)	18286(5)	30(1)
Br(1)	-40050(12)	48913(6)	21590(6)	56(1)
Br(2)	7027(14)	11887(8)	44891(5)	67(1)
Br(3)	-45445(12)	-1136(7)	10203(7)	61(1)
Cl	-435(2)	2612(1)	731(1)	34(1)
N(1)	2020(7)	3111(4)	1649(4)	34(2)
N(2)	1026(7)	3041(4)	2003(3)	35(2)
N(3)	1930(7)	1686(4)	1273(3)	31(2)
N(4)	991(8)	1533(4)	1636(4)	35(2)
N(7)	-1920(7)	3041(4)	1998(3)	32(2)
N(8)	-2829(7)	2829(4)	2373(3)	32(2)
N(9)	-353(7)	1947(5)	2791(4)	36(2)
N(10)	-1553(7)	1868(4)	2998(3)	33(2)
N(11)	-2053(7)	1497(4)	1649(3)	32(2)
N(12)	-2992(7)	1527(4)	2042(3)	33(2)
B	-2859(11)	2032(6)	2596(5)	34(2)
C(1)	2963(9)	3546(6)	1942(5)	40(2)
C(2)	2564(10)	3775(6)	2477(5)	47(3)
C(3)	1354(9)	3445(6)	2498(4)	37(2)
C(4)	2735(11)	1110(6)	1279(5)	50(3)
C(5)	2340(11)	582(6)	1641(6)	56(3)
C(6)	1228(10)	868(6)	1862(5)	47(3)
C(10)	2018(10)	2557(6)	-173(4)	39(2)
C(11)	1896(10)	3319(5)	4(4)	37(2)
C(12)	3038(11)	3500(5)	394(4)	41(2)
C(13)	3871(10)	2875(6)	511(4)	40(2)
C(14)	3244(9)	2310(6)	122(4)	34(2)
C(15)	1062(11)	2159(7)	-614(5)	52(3)
C(16)	790(12)	3798(7)	-242(5)	57(3)
C(17)	3386(15)	4243(6)	637(6)	66(4)
C(18)	5212(10)	2804(6)	854(5)	47(3)
C(19)	3845(13)	1599(6)	3(5)	54(3)
C(20)	-2124(9)	3761(5)	1885(4)	33(2)
C(21)	-3220(9)	3986(5)	2179(4)	34(2)
C(22)	-3614(9)	3382(5)	2485(4)	34(2)
C(23)	-1343(9)	4166(5)	1473(5)	38(2)
C(24)	-2188(11)	4359(6)	873(5)	48(3)
C(25)	-699(11)	4850(6)	1778(5)	50(3)
C(26)	-1389(9)	1616(5)	3565(4)	34(2)
C(27)	-85(11)	1548(6)	3737(4)	42(2)
C(28)	563(10)	1757(6)	3247(4)	41(2)
C(29)	2034(11)	1799(8)	3190(6)	68(4)
C(30)	2668(15)	2357(11)	3647(7)	110(7)
C(31)	2716(14)	1070(9)	3295(7)	87(5)
C(32)	-3914(9)	1022(5)	1897(5)	37(2)
C(33)	-3565(9)	657(5)	1397(5)	39(2)
C(34)	-2409(10)	975(5)	1250(4)	38(2)
C(35)	-1605(10)	799(6)	742(5)	46(3)
C(36)	-1164(12)	-4(6)	769(6)	60(3)
C(37)	-2344(13)	966(8)	129(5)	68(4)

^a Equivalent isotropic U defined as one-third of the trace of the orthogonalized U_{ij} tensor.

them. However, the ^1H NMR spectra of the paramagnetic octahedral Co(II) complexes were quite informative. The peak assignment was done on the basis of the known relationship among observed chemical shifts, the cosine of the H–Co–B angle, and the Co–H distance, resulting in substantial upfield or downfield shifts of the respective protons.^{2,3} Thus, for example, the spectrum of complex **6** (Figure 1), besides the C_5Me_5 signal at 14.6 ppm, showed peaks at -16.5, -37.2, and -38.1 ppm (6:6:6 ratio) assigned to the unique isopropyl group *trans* to the Cl atom and to the inner and outer methyls of the two remaining isopropyl groups, respectively. The assignment of the “h” and “i” methyl peaks was based on these methyls being closer to Co than the “g” methyls (due to the tighter Ir–Cl–Co bridge) and hence subject to greater shifts. There were two types of H5 and $\text{CH}(\text{CH}_3)_2$ protons for the $\text{HB}(3\text{-}i\text{-pr-4-Br-pz})_3$ ligand, each in a 2:1 ratio. All these data were consistent

Table 3. Final Atomic Coordinates ($\times 10^4$; $\times 10^5$ for Ru, Ni, and Br Atoms) and Equivalent Isotropic Displacement Parameters ($\text{\AA}^2 \times 10^3$) for **12**

atom	x	y	z	$U(\text{eq})^a$
Ru	-9147(3)	50000	9251(3)	26(1)
Ni	-14621(5)	42167(3)	-4993(4)	23(1)
Br(1)	35471(7)	57330(3)	-40756(7)	73(1)
Br(2)	-9297(6)	20143(2)	-42325(4)	46(1)
Br(3)	68539(5)	28957(2)	20889(4)	41(1)
N(1)	-1376(3)	4853(1)	-1024(3)	29(1)
N(2)	-452(3)	4619(1)	-1508(3)	26(1)
N(3)	-354(4)	4059(1)	1072(3)	28(1)
N(4)	591(4)	2797(2)	631(3)	26(1)
N(5)	1216(3)	5233(2)	1181(3)	26(1)
N(6)	2052(3)	4947(2)	670(3)	27(1)
N(7)	2430(4)	4627(2)	-1728(3)	29(1)
N(8)	3237(3)	4242(2)	-2107(3)	32(1)
N(9)	948(4)	3409(2)	-1783(3)	29(1)
N(10)	2014(4)	3235(2)	-2180(3)	30(1)
N(11)	3483(4)	3775(2)	475(3)	27(1)
N(12)	4142(4)	3521(2)	-256(3)	28(1)
C(1)	-2610(4)	4982(2)	-2007(4)	38(1)
C(2)	-2469(5)	4840(2)	-3123(4)	40(1)
C(3)	-1097(5)	4612(2)	-2761(4)	34(1)
C(4)	-834(5)	3607(2)	1606(4)	39(1)
C(5)	-221(5)	3054(2)	1533(4)	39(1)
C(6)	670(5)	3199(2)	917(4)	31(1)
C(7)	1990(5)	5707(2)	1885(4)	38(1)
C(8)	3312(5)	5728(2)	1817(5)	42(1)
C(9)	3304(4)	5240(2)	1055(4)	34(1)
C(10)	-2411(5)	5812(2)	553(5)	39(1)
C(11)	-1168(5)	5924(2)	1611(4)	36(1)
C(12)	-688(5)	5514(2)	2651(4)	40(1)
C(13)	-1418(5)	4968(2)	2683(4)	44(1)
C(14)	-2670(5)	4838(2)	1583(5)	45(1)
C(5)	-3148(5)	5241(2)	564(5)	42(1)
C(16)	-2941(6)	6275(2)	-503(5)	50(1)
C(17)	-1820(7)	6472(3)	-1009(6)	63(2)
C(18)	-3544(8)	6839(3)	-53(7)	82(2)
C(19)	-906(7)	4571(3)	3835(5)	63(2)
C(20)	2403(4)	5175(2)	-2282(4)	36(1)
C(21)	3195(5)	5124(2)	-3049(4)	43(1)
C(22)	3700(5)	4537(2)	-2926(4)	42(1)
C(23)	1649(5)	5732(2)	-2030(5)	45(1)
C(24)	2692(7)	6253(3)	-1419(6)	66(2)
C(25)	453(6)	5957(3)	-3230(6)	60(2)
C(26)	1562(5)	2768(2)	-3011(4)	36(1)
C(27)	188(5)	2635(2)	-3152(4)	33(1)
C(28)	-183(4)	3040(2)	-2370(3)	28(1)
C(29)	-1569(4)	3081(2)	-2164(4)	34(1)
C(30)	-2824(5)	3231(2)	-3401(5)	46(1)
C(31)	-1880(6)	2487(2)	-1602(5)	49(1)
C(32)	5322(4)	3222(2)	472(4)	31(1)
C(33)	5436(4)	3277(2)	1695(4)	30(1)
C(34)	4274(4)	3636(2)	1682(4)	28(1)
C(35)	3892(5)	3860(2)	2759(4)	36(1)
C(36)	3675(6)	3323(3)	3558(5)	54(2)
C(37)	5044(5)	4302(2)	3615(4)	48(1)
B	3472(5)	3561(2)	-1707(4)	29(1)
C(1S)	3543(11)	1285(5)	5027(9)	139(5)
Cl(1)	2810(2)	1150(1)	6111(2)	87(1)
Cl(2)	4716(3)	1870(1)	5320(3)	116(1)

^a Equivalent isotropic U defined as one-third of the trace of the orthogonalized U_{ij} tensor.

with the presence of a triple Cl, pz, pz bridge between the two metal atoms and indicated that the rotation of the isopropyl groups around the C3(heterocycle)–CH bond was hindered. The formation of the IrCo complex **6** was also accomplished by reacting $[\text{Ir}(\eta^5\text{-C}_5\text{Me}_5)\text{Cl}(\text{Hpz})_2]\text{BF}_4$, **4**, and KOH, in 80% yield. The structural characterization of this type of complex was completed by a single-crystal X-ray analysis of compound **6** (see below).

A similar reaction between the related ($\eta^6\text{-}p\text{-cymene}$)-ruthenium complex $[\text{Ru}(\eta^6\text{-}p\text{-cymene})(\text{pz})_2(\text{Hpz})]$ (**2**) and **4** or

Table 4. Final Atomic Coordinates ($\times 10^4$; $\times 10^5$ for Ir, Ni, and Br Atoms) and Equivalent Isotropic Displacement Parameters ($\text{\AA}^2 \times 10^3$) for **13**

atom	x	y	z	$U(\text{eq})^a$
Ir	15(2)	15918(1)	40(2)	19(1)
Ni	-5559(6)	18610(3)	27042(6)	20(1)
Br(1)	-46532(6)	13417(4)	40473(7)	45(1)
Br(2)	-2283(8)	39595(3)	41689(7)	51(1)
Br(3)	16493(7)	7804(4)	63254(7)	51(1)
B	1036(5)	2094(3)	4967(6)	23(2)
N(1)	-1076(4)	2060(2)	509(4)	24(1)
N(2)	-1334(4)	2112(2)	1465(4)	23(1)
N(3)	972(4)	1882(4)	1134(4)	24(1)
N(4)	731(4)	2010(2)	2071(4)	23(1)
N(5)	-267(5)	1095(2)	1142(4)	22(1)
N(6)	-548(4)	1197(2)	2081(4)	23(1)
N(7)	-891(4)	1715(2)	3421(4)	23(1)
N(8)	-1935(4)	1877(2)	4387(4)	25(1)
N(9)	-565(4)	2553(2)	3436(4)	23(1)
N(10)	-734(4)	2550(2)	4432(4)	22(1)
N(11)	241(5)	1599(2)	4148(4)	24(1)
N(12)	-178(4)	1739(2)	4986(5)	26(1)
C(1)	-1664(7)	2344(3)	-74(6)	43(2)
C(2)	-2326(6)	2578(3)	497(6)	38(2)
C(3)	-2082(5)	2416(3)	1451(6)	30(2)
C(4)	1935(6)	1952(3)	1090(6)	40(2)
C(5)	2336(5)	2125(3)	1984(6)	40(2)
C(6)	1554(5)	2157(3)	2578(5)	29(2)
C(7)	-201(6)	621(3)	1068(6)	35(2)
C(8)	-431(6)	398(3)	1956(6)	36(2)
C(9)	-653(5)	787(3)	2552(5)	30(2)
C(10)	1985(6)	1831(4)	-1341(6)	50(2)
C(11)	-269(6)	1084(3)	-1243(5)	30(2)
C(12)	-684(6)	1525(3)	-1528(5)	27(2)
C(13)	91(5)	1877(3)	-1512(5)	25(1)
C(14)	973(6)	1627(3)	-1242(5)	29(2)
C(15)	1512(7)	757(4)	-815(7)	51(2)
C(16)	-839(7)	628(3)	-1288(6)	43(2)
C(17)	-1734(6)	1588(3)	-1925(7)	40(2)
C(18)	49(7)	2380(3)	-1901(6)	43(2)
C(19)	1985(6)	1831(4)	-1341(6)	49(2)
C(20)	-2768(5)	1522(3)	3151(6)	26(1)
C(21)	-3362(5)	1556(3)	964(6)	30(2)
C(22)	-2812(5)	1785(3)	4737(6)	31(2)
C(23)	-3001(5)	1308(3)	2124(6)	33(2)
C(24)	-3198(7)	778(3)	2158(7)	48(2)
C(25)	-3868(6)	1577(4)	1563(7)	44(2)
C(26)	-639(5)	3002(3)	4811(6)	30(2)
C(27)	-402(5)	3291(2)	4040(6)	26(2)
C(28)	-374(5)	3010(3)	3175(5)	26(1)
C(29)	-188(5)	3156(3)	2133(6)	28(2)
C(30)	-952(6)	3519(3)	1731(6)	37(2)
C(31)	845(6)	3362(3)	2080(7)	37(2)
C(32)	204(6)	1500(3)	5802(6)	30(2)
C(33)	907(5)	1201(3)	5467(5)	29(2)
C(34)	921(5)	1271(3)	4428(5)	24(1)
C(35)	1605(5)	1054(3)	3719(5)	29(2)
C(36)	2656(5)	1214(3)	3984(6)	38(2)
C(37)	1572(6)	509(3)	3733(7)	44(2)
C(100)	-823(8)	4683(4)	6429(8)	62(3)
Cl(1)	-1661(4)	4219(2)	6449(3)	116(2)
Cl(2)	-1058(4)	5053(1)	5387(3)	98(1)
Cl(3)	-722(3)	4993(2)	7553(3)	105(1)
C(101)	-2397(8)	-218(4)	631(9)	61(3)
Cl(4)	-3098(3)	-23(2)	-442(3)	90(1)
Cl(5)	-1479(3)	-609(1)	319(3)	86(1)
Cl(6)	-3154(2)	-487(1)	-1478(3)	78(1)

^a Equivalent isotropic U defined as one-third of the trace of the orthogonalized U_{ij} tensor.

5 gave, in both cases, the expected bis(μ -pyrazolato) μ -chloro complexes $[(\eta^6\text{-}p\text{-cymene})\text{Ru}(\mu\text{-pz})_2(\mu\text{-Cl})\text{M}'\{\text{HB}(3\text{-}i\text{-Pr-4-Br-pz})_3\}]$ ($\text{M}' = \text{Co}$ (**9**), Ni (**10**)) but contaminated by the triply pyrazolato-bridged compounds $[(\eta^6\text{-}p\text{-cymene})\text{Ru}(\mu\text{-pz})_3\text{M}'\{\text{HB}(3\text{-}i\text{-Pr-4-Br-pz})_3\}]$ ($\text{M}' = \text{Co}$ (**11**), Ni (**12**)). From the mixtures, the four molecular ion peaks have been detected by

FAB⁺ mass spectrometry, and significant proton resonances were assigned by ¹H NMR spectroscopy for the cobalt complexes.

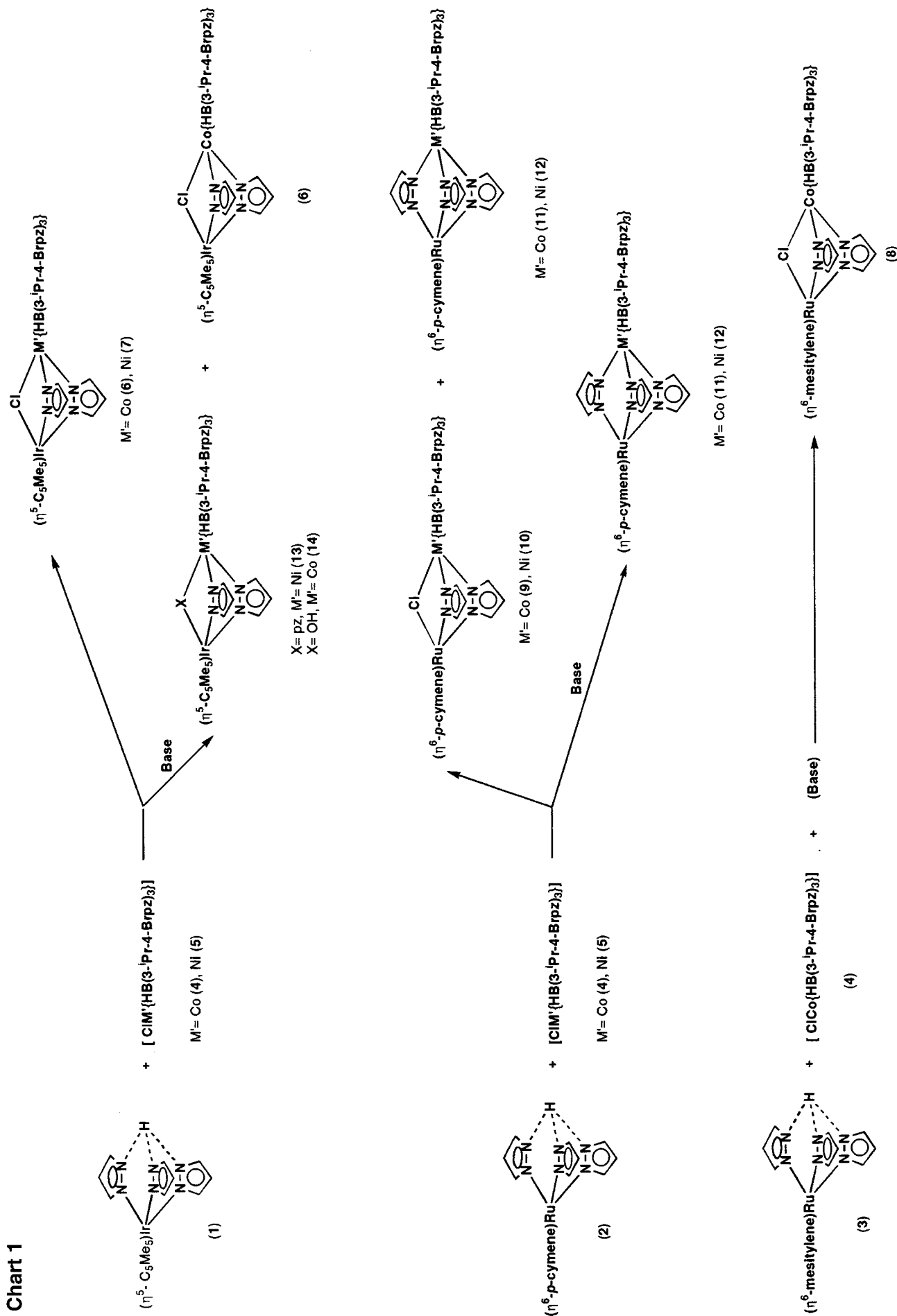
When the aforementioned reaction was carried out in the presence of bases, such as NEt_3 or KOH , the triply pyrazolato-bridged complexes **11** and **12** were obtained as unique products. The ¹H NMR spectrum of **11** showed only one signal, at -36.2 ppm, for the 18 methyl isopropyl protons of the poly(pyrazolyl)borate ligand, as expected for a molecule with C_{3v} symmetry. The existence of a triple pyrazolate bridge is a usual structural feature in the chemistry of tris(pyrazolyl)borato transition-metal complexes¹ but extremely rare in bi- or polynuclear pyrazolato-bridged transition-metal compounds.^{8,18} In order to provide conclusive evidence for the existence of this kind of bridge, single crystals of complex **12** were grown by slow diffusion of hexane into a dichloromethane solution, and its structure was determined by an X-ray diffraction study (see below). Analogously, the reaction of the iridium ligand **1** with **5** and KOH ¹⁹ afforded a pyrazolato-bridged IrNi complex (**13**). The elemental analysis was consistent with a triply pyrazolato-bridged species $[(\eta^5\text{-C}_5\text{Me}_5)\text{Ir}(\mu\text{-pz})_3\text{Ni}\{\text{HB}(3\text{-}i\text{-Pr-4-Br-pz})_3\}]$, while the most significant FAB⁺ MS spectrum peak appeared at $m/z = 1095$ with an isotopic distribution which corresponded to a doubly bridged complex $[(\eta^5\text{-C}_5\text{Me}_5)\text{Ir}(\text{pz})_2\text{Ni}\{\text{HB}(3\text{-}i\text{-Pr-4-Br-pz})_3\}]^+$. An X-ray structural analysis revealed the former formulation to be correct (see below).

In contrast with the formation of **13**, complex **1** reacted with **4** and KOH (molar ratio 1:1:1), yielding approximately equal amounts of **6** and the μ -hydroxo IrCo compound $[(\eta^5\text{-C}_5\text{Me}_5)\text{Ir}(\mu\text{-pz})_2(\mu\text{-OH})\text{Co}\{\text{HB}(3\text{-}i\text{-Pr-4-Br-pz})_3\}]$ (**14**). When excess KOH was used (molar ratio 1:1:2), the proportion of complex **14** increased up to 94%. Although we have not been able to further purify **14**, its spectroscopic data were in good agreement with those expected for the μ -hydroxo derivative. Thus, the ¹H NMR spectrum, which spanned almost 250 ppm, accounted for every proton of each ligand. The signals for the isopropyl methyl groups, which appeared in a 6:6:6 ratio at -32.6 , -33.9 , and -41.1 ppm, were consistent with the presence of a triple OH, pz, pz bridge between the two metal atoms and indicated that the rotation of the isopropyl groups is again hindered. The FAB⁺ MS spectrum showed a peak at $m/z = 1113$ attributable to the molecular ion, and the IR spectrum showed a weak band at 3640 cm^{-1} for the $\nu(\text{OH})$ vibration. Attempts to obtain the triply pyrazolato-bridged complex $[(\eta^5\text{-C}_5\text{Me}_5)\text{Ir}(\mu\text{-pz})_3\text{Co}\{\text{HB}(3\text{-}i\text{-Pr-4-Br-pz})_3\}]$ using a stronger base, such as ⁿBuLi, afforded complex **6**, in 35% yield, as the sole identified product.

Additionally, the EPR spectra of compounds **6**, **7**, and **11-14** have been measured. In all cases, a broad absorption, which spanned from zero magnetic field to 0.8 T, was detected. A narrower signal was also present in some cases, at $g \approx 2.2-2.4$ with a peak to peak width of $\Delta H_{pp} \approx 10$ mT in the case of compounds **6** and **7** and at $g \approx 2$ with $\Delta H_{pp} \approx 30$ mT for compounds **12** and **14**. Furthermore, the absence of any correlation between the spectral modifications and the change of the paramagnetic metal indicates that the magnetic electron (unpaired electron) is likely delocalized along the skeleton of the molecule but not localized at any particular metal center. Complex **12** was selected as a representative organometallic example for the study of the magnetic behavior. The results are those expected for an octahedral Ni(II) complex with two

- (18) (a) Chong, K. S.; Rettig, S. J.; Storr, A.; Trotter, J. *Can. J. Chem.* **1979**, *57*, 3099. (b) Trofimenko, S. *J. Am. Chem. Soc.* **1969**, *91*, 5410.
 (19) The presence of NEt_3 in the reaction between **1** and **4** or **5** did not produce any significant change in the course of the reaction, complexes **6** and **7** being formed in yields similar to those obtained in the absence of the base.

Chart 1



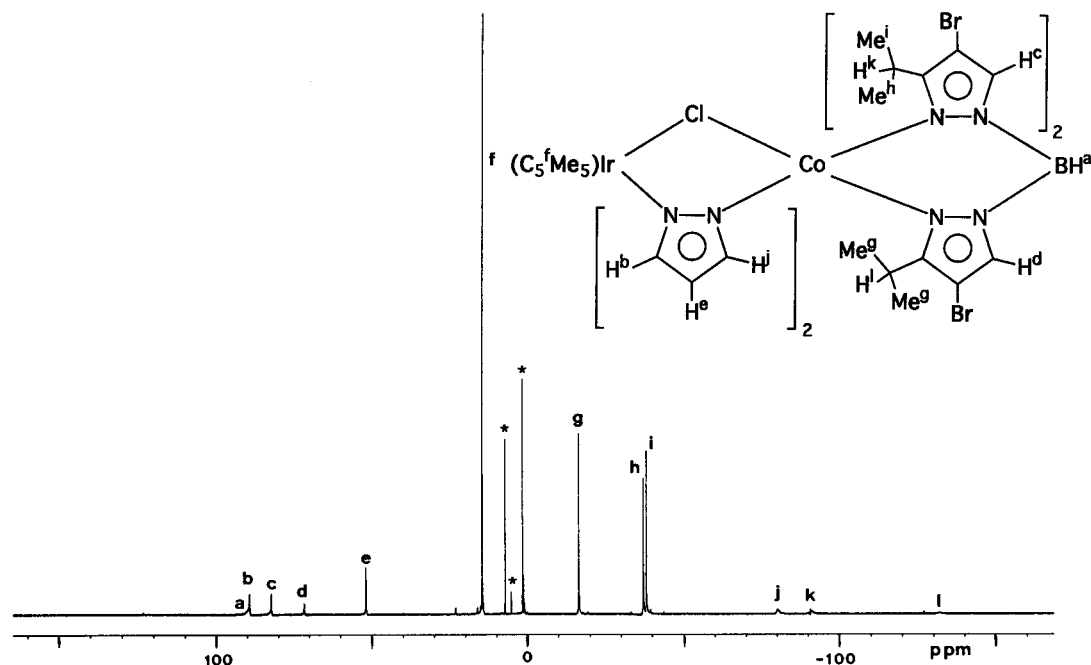


Figure 1. ^1H NMR spectrum of **6**. The asterisks denote solvents.

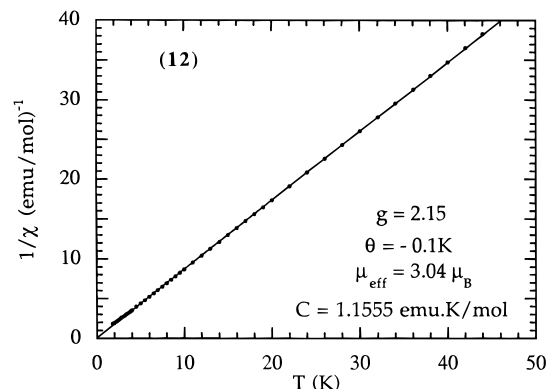


Figure 2. Evolution of the inverse of the dc magnetic susceptibility of complex **12** as a function of temperature.

unpaired electrons.²⁰ The susceptibility data, after corrections from diamagnetic contributions and some temperature independent paramagnetism, fitted well to a Curie–Weiss law with $C = 1.1555$ (emu·K)/mol and $\Theta = -0.1$ K. This gives $\mu_{\text{eff}} = 3.04 \mu_{\text{B}}$. In Figure 2, the temperature dependence of the inverse of the susceptibility is depicted. Additional magnetization measurements at 1.8 and 3.0 K confirmed the susceptibility results. The magnetization of **12** tends to saturate at $2.15 \mu_{\text{B}}$ /molecule. This value agrees well with an $S = 1$ ground state and $g = 2.15$.

Molecular Structures of $[(\eta^5\text{-C}_5\text{Me}_5)\text{Ir}(\mu\text{-pz})_2(\mu\text{-Cl})\text{Co}\{\text{HB}(3\text{-}i\text{-Pr-4-Br-pz})_3\}]$ (**6**), $[(\eta^6\text{-}p\text{-cymene})\text{Ru}(\mu\text{-pz})_3\text{Ni}\{\text{HB}(3\text{-}i\text{-Pr-4-Br-pz})_3\}]$ (**12**), and $[(\eta^5\text{-C}_5\text{Me}_5)\text{Ir}(\mu\text{-pz})_3\text{Ni}\{\text{HB}(3\text{-}i\text{-Pr-4-Br-pz})_3\}]$ (**13**). The neutral complexes **6**, **12**, and **13** consist of linear $\text{M}\cdots\text{M}'\cdots\text{B}$ backbones with bridging pyrazolate groups coordinating the dimetallic $\text{M}\cdots\text{M}'$ unit and the $\text{M}'\cdots\text{B}$ moiety ($\text{M} = \text{Ir}$ (**6** and **13**), Ru (**12**); $\text{M}' = \text{Co}$ (**6**), Ni (**12** and **13**)). For complex **6** (Figure 3), two pyrazolate anions and a bridging chloride ligand engage the dimetallic unit ($\text{Ir}\cdots\text{Co}$), while for complexes **12** and **13** (Figures 4 and 5, respectively), the two metals are triply bridged by unsubstituted pyrazolate ligands ($\mu\text{-pz}$). In each complex the $\text{HB}(3\text{-}i\text{-Pr-4-Br-pz})_3$ ligand

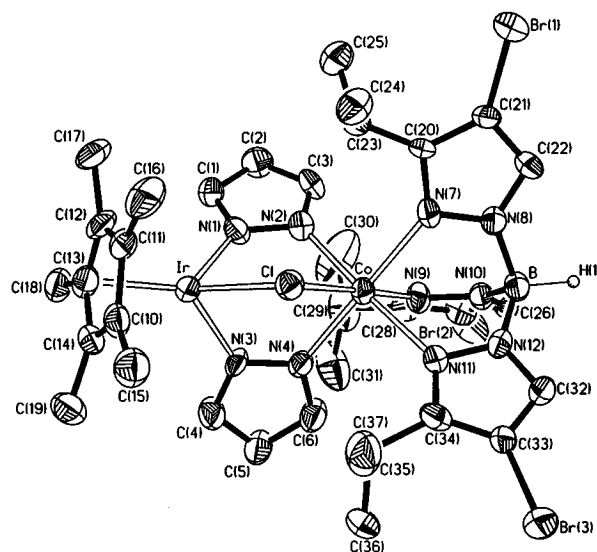


Figure 3. Molecular structure of **6** with atoms represented as 50% probability ellipsoids. All hydrogens have been omitted for clarity, excluding the refined hydrogen bonded to the boron.

is tridentate. The coordination sphere for the central metal M' (Co or Ni) is in all cases octahedral, while for M (Ru or Ir) it is that described as a pseudooctahedral “three-legged piano stool”, with the coordination completed by a $\eta^5\text{-C}_5\text{Me}_5$ group (**6** and **13**) or a $\eta^6\text{-}p\text{-cymene}$ ligand (**12**). The boron environment in each complex describes the expected tetrahedron, formed from three nitrogen atoms of the 4-bromo-3-isopropylpyrazolate groups and a terminal hydrogen.

In complex **6**, the $\text{Ir}\text{-C}_5\text{Me}_5$ metal–carbon distances (mean $2.156(4)$ Å) and the corresponding $\text{Ir}\text{-C}_5\text{Me}_5$ (centroid) length ($1.78(1)$ Å) are similar to those observed in related mononuclear iridium complexes, as in $[(\eta^5\text{-C}_5\text{Me}_5)\text{IrCl}(\text{bipy})]^+$,²¹ $[(\eta^5\text{-C}_5\text{Me}_5)\text{IrCl}(\text{biimidazole})]^+$,²² or $[(\eta^5\text{-C}_5\text{Me}_5)\text{IrCl}(\text{bipy}')]^+$ ²³ ($\text{Ir}\text{-C}$

(21) Youinou, M. T.; Ziessel, R. *J. Organomet. Chem.* **1989**, *363*, 197.

(22) Ziessel, R.; Youinou, M. T.; Balgroune, F.; Grandjean, D. *J. Organomet. Chem.* **1992**, *441*, 143.

(23) Ziessel, R.; Noblat-Chardon, S.; Deronzier, A.; Matt, D.; Toupet, L.; Balgroune, F.; Grandjean, D. *Acta Crystallogr.* **1993**, *B49*, 515.

(20) *Encyclopedia of Inorganic Chemistry*; King, R. B., Ed.; John Wiley and Sons: Chichester, U.K., 1994; Vol. 5, p 2395.

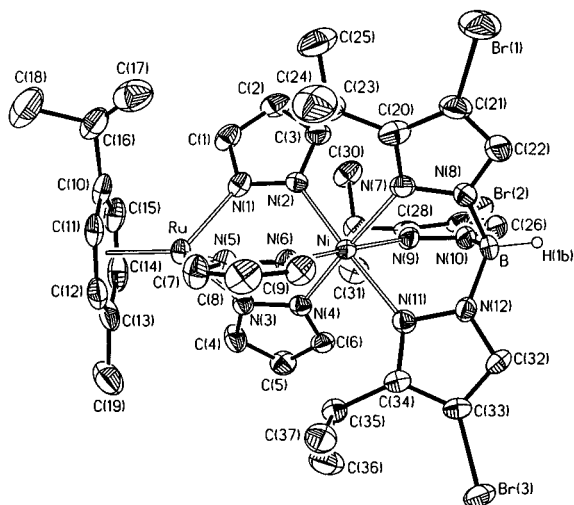


Figure 4. Molecular representation of **12** with the atom-labeling scheme used. Hydrogens have been omitted for clarity.

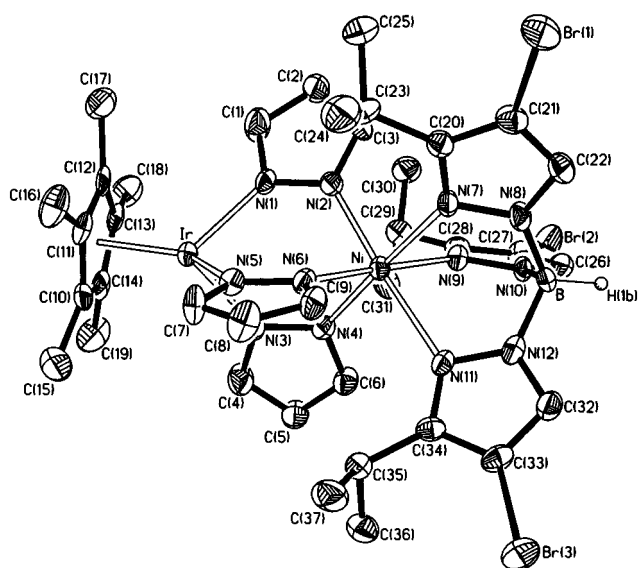


Figure 5. Molecular structure of **13** with the atom-labeling scheme used.

mean distances 2.155(5), 2.149(4), and 2.168(1) Å, respectively; $\text{bipy}' = 3\text{-}((1\text{-pyrrolyl})\text{propyl})\text{-}2,2'\text{-bipyridine-}4,4'\text{-dicarboxylate}$) or in the analogous dinuclear pyrazolate–chloride mixed-bridge rhodium complex $[(\eta^5\text{-C}_5\text{Me}_5)\text{Rh}(\mu\text{-pz})_2(\mu\text{-Cl})\text{Rh}(\eta^5\text{-C}_5\text{Me}_5)]^+$ ($\text{Rh}\text{-C}_5\text{Me}_5(\text{centroid})$ 1.777(2) Å).²⁴

Interestingly, when the chloride bridge in **6** is substituted by a third bridging pyrazolate ligand, that is complex **13**, these distances involved in the $\text{Ir}\text{-C}_5\text{Me}_5$ interaction are significantly lengthened to 2.192(4) ($\text{Ir}\text{-C}$) and 1.827(7) Å ($\text{Ir}\text{-C}_5\text{Me}_5$), probably as a result of the presence of the more sterically demanding bridging pyrazolate. This fact is also evidence if we compare the closely related doubly-bridged complex $[(\eta^5\text{-C}_5\text{Me}_5)\text{Ir}(\text{pz})(\mu\text{-pz})_2\text{Ag}(\text{PPh}_3)]$ (1.808(2) Å)⁷ and the unique previously-described iridium compound with a triple pyrazolate bridge $[(\eta^5\text{-C}_5\text{Me}_5)\text{Ir}(\mu\text{-pz})_3\text{Rh}(\text{OOH})(\text{dppe})]^+$ (1.829(7) Å).⁸

The $\text{Ir}\text{-N}$ bond distances in **6** (mean 2.070(5) Å) are significantly shorter than those found in **13** (mean 2.109(4) Å) in agreement with the proposed expansion of the iridium coordination environment when a third pyrazolate bridging ligand is included. It is noteworthy that the above mentioned

Table 5. Selected Bond Distances (Å) and Angles (deg) for Complexes **6**, **12**, and **13**

	complex (M/M')		
	6 (Ir/Co)	12 (Ru/Ni)	13 (Ir/Ni)
M–N(1)	2.076(8)	2.117(4)	2.119(6)
M–N(3)	2.065(7)	2.106(3)	2.099(5)
M–N(5)/Cl ^a	2.437(2)	2.123(4)	2.108(6)
M–C(10)	2.160(9)	2.256(4)	2.180(8)
M–C(11)	2.144(9)	2.202(4)	2.196(7)
M–C(12)	2.161(9)	2.200(4)	2.194(6)
M–C(13)	2.13(1)	2.251(4)	2.184(6)
M–C(14)	2.178(9)	2.202(4)	2.204(7)
M–C(15)		2.201(4)	
M–G ^b	1.78(1)	1.710(6)	1.827(7)
M'–N(2)	2.054(8)	2.038(3)	2.026(6)
M'–N(4)	2.068(8)	2.033(4)	2.050(6)
M'–N(6)/Cl ^c	2.516(3)	2.013(3)	2.032(6)
M'–N(7)	2.141(8)	2.178(4)	2.163(6)
M'–N(9)	2.208(8)	2.212(3)	2.164(6)
M'–N(11)	2.173(8)	2.149(3)	2.265(6)
B–N(8)	1.55(1)	1.540(6)	1.532(9)
B–N(10)	1.53(1)	1.537(6)	1.53(1)
B–N(12)	1.53(1)	1.534(6)	1.536(9)
M...M'...B	172.0(2)	179.74(9)	179.5(2)
N(1)–M–N(3)	83.4(3)	83.3(1)	87.3(2)
N(1)–M–N(5)/Cl ^a	88.1(2)	89.4(1)	90.9(2)
N(3)–M–N(5)/Cl ^a	85.4(2)	89.5(1)	82.6(2)
G–M–N(1)	129.7(4)	128.2(2)	125.4(3)
G–M–N(3)	132.9(4)	128.6(2)	130.6(3)
G–M–N(5)/Cl ^a	122.3(3)	124.5(2)	126.2(3)
Ir–Cl–Co	94.13(9)		
N(2)–M'–N(4)	89.2(3)	90.2(1)	90.6(2)
N(2)–M'–N(6)/Cl ^c	85.4(2)	91.0(1)	90.0(2)
N(4)–M'–N(6)/Cl ^c	83.0(2)	91.3(1)	89.2(2)
N(7)–M'–N(9)	87.1(2)	87.1(1)	86.3(2)
N(7)–M'–N(11)	86.2(2)	86.8(1)	86.2(2)
N(9)–M'–N(11)	86.2(2)	85.9(1)	85.5(2)
N(8)–B–N(10)	108.7(8)	108.6(1)	109.2(5)
N(8)–B–N(12)	108.7(7)	110.2(3)	109.7(5)
N(10)–B–N(12)	109.1(7)	109.1(4)	108.2(5)

^a Bond and angles involving Cl (**6**) or N(5) (**12** and **13**). ^b G Represents the centroid for ($\eta^5\text{-C}_5\text{Me}_5$) (**6** and **13**) and $\eta^6\text{-p-cymene}$ (**12**). ^c Bond and angles involving Cl (**6**) or N(6) (**12** and **13**).

bond distances are close to the limiting bond lengths so far encountered in other binuclear pyrazolato-bridged ($\eta^5\text{-C}_5\text{Me}_5$)- Ir^{III} complexes, which range from 2.074(6) to 2.106(4) Å.^{8,25} As is usual for the case of bridging chloride ligands, the $\text{Ir}\text{-Cl}$ bond length observed in **6** is slightly longer, 2.437(2) Å, than the values reported for terminal chloride ligands in related complexes of the type $[(\eta^5\text{-C}_5\text{Me}_5)\text{IrCl}(\text{N-N})]$ ($\text{N-N} = \text{bipy}$, 2.404(2) Å, or biimidazole, 2.394(2) Å).^{21–23}

As observed in **13**, the existence of *three* bridging pyrazolate groups in **12** yields $\text{Ru}\text{-N}$ distances (range 2.106(3)–2.123(4) Å) longer than those previously reported in *p-cymene*–ruthenium complexes containing *one* or *two* bridging pyrazolate ligands such as $[(p\text{-cymene})\text{Ru}(\mu\text{-pz})(\mu\text{-Cl})_2\text{Rh}(\text{tfb})]$ ($\text{tfb} = 5,6,7,8\text{-tetrafluoro-}1,4\text{-dihydro-}1,4\text{-ethenonaphthalene}$) (2.096(6) Å),²⁶ $[(p\text{-cymene})\text{ClRu}(\mu\text{-pz})_2\text{M}(\text{CO})_2]$ ($\text{M} = \text{Ir}$, 2.079(4) and 2.088(4) Å; $\text{M} = \text{Rh}$, 2.086(3) and 2.086(3) Å),²⁷ $[(p\text{-cymene})\text{Ru}(\mu\text{-pz})_2\text{IrCl}(\text{CO})_2]$ (2.075(6) and 2.083(5) Å),²⁷ $[(p\text{-cymene})\text{Ru}]_2(\mu\text{-pz})_2(\mu\text{-OH})\text{BPh}_4$ (2.086(2) Å),²⁸ and $[(p\text{-cymene})(\text{Hpz})\text{Ru}(\mu\text{-pz})_2\text{Ir}(\text{CO})_2]$ (2.093(5) and 2.088(4) Å).⁹ In

(25) Carmona, D.; Ferrer, J.; Lahoz, F. J.; Oro, L. A.; Reyes, J.; Esteban, M. *J. Chem. Soc., Dalton Trans.* **1991**, 2811.

(26) Oro, L. A.; Carmona, D.; García, M. P.; Lahoz, F. J.; Reyes, J.; Foces-Foces, C.; Cano, F. H. *J. Organomet. Chem.* **1985**, *C43*, 296.

(27) Carmona, D.; Ferrer, J.; Mendoza, A.; Lahoz, F. J.; Reyes, J.; Oro, L. A.; *Angew. Chem., Int. Ed. Engl.* **1991**, *30*, 1171.

(28) Oro, L. A.; García, M. P.; Carmona, D.; Foces-Foces, C.; Cano, F. H. *Inorg. Chim. Acta* **1985**, *96*, L21.

(24) Bailey, J. A.; Grundy, S. L.; Stobart, S. R. *Organometallics* **1990**, *9*, 536.

a similar way, the Ru–C distances observed for the arene ligand in **12** (mean 2.211(2) Å) and the derived Ru–*p*-cymene-(centroid) separation (1.710(6) Å) are clearly elongated if compared to the usual values reported in (*p*-cymene)(μ -pyrazolato)ruthenium complexes (Ru–*p*-cymene distance range 1.662–1.697(5) Å).^{5,9,26–28}

The cobalt coordination environment in **6** exhibits the expected distorted octahedron. Apart from the bridging unsubstituted pyrazolates (mean Co–N 2.061(6) Å) and the chloride anion (Co–Cl 2.516(3) Å), three further cobalt–nitrogen bonds from the bridging 4-bromo-3-isopropylpyrazolate groups of the poly(pyrazolyl)borate ligand (mean 2.174(5) Å) complete the octahedral coordination. The shortest Co–N bond lengths, to N(2) and N(4) (Figure 3), are shorter than those found in the homoleptic complex [Co{HBpz₃}₂] (2.130(7) Å).²⁹ The longest Co–N separations observed in **6** compare well with those reported for related poly(pyrazolyl)borato–cobalt(II) complexes when a relatively bulky substituent is linked to the pyrazolate ring in the relative 3-position, as in [Co{HB(3-*i*-Pr-pz)₂(5-*i*-Pr-pz)}₂] (2.164(2) and 2.170(1) Å) or [Co{HB(3-*i*-Pr-4-Br-pz)₂(5-*i*-Pr-4-Br-pz)}₂] (2.150 and 2.208(3) Å).²

The nickel environment in **12** resembles a slightly distorted octahedron, consisting of three Ni–N bonds from the bridging unsubstituted pyrazolate ligands (mean 2.028(2) Å) and three further Ni–N links from the bridging 4-bromo-3-isopropylpyrazolate groups which connect the Ni and B atoms (mean 2.180(2) Å). An equivalent situation is observed in **13** with remarkable differences in the Ni–N lengths at both sides of the metal center, 2.036(4) and 2.197(4) Å. For complexes **12** and **13**, the nickel–boron segments are found to be structurally identical to that observed in [Ni{HB(μ -3-*i*-Pr-4-Br-pz)₃}{HB(μ -pz)₃}], although the differences of the Ni–N bond distances at both sides of the metal coordination sphere are not so remarkable (2.078(4) and 2.151(4) Å).³

The M···M' separations are found to be 3.627(2), 3.777(1), and 3.807(1) Å for **6**, **12**, and **13**, respectively, and hence no metal–metal interaction is invoked. The M···M'···B backbone is essentially linear, with respective angles of 172.0(2), 179.74(9), and 179.53(15)°. Clearly, in the case of **6**, the presence of the chloride bridge across the dimetallic skeleton allows a slight modification of the linear nature of the backbone, which collapses slightly, relieving pyrazolate–pyrazolate repulsions. The bridging pyrazolate ligands in all the three complexes are in the expected staggered conformations (Figure 6), analogous to that reported for [Ni{HB(μ -3-*i*-Pr-4-Br-pz)₃}{HB(μ -pz)₃}], which contains two different sets of three equivalent pyrazolates and a slightly trigonal-distorted metal environment.³ For **12** and **13**, the dihedral angles between the two sets of three pyrazolate groups amount to the expected essentially symmetrical 120° distribution.^{8,18a} However, in **6**, the distribution around the dimetallic unit is modified, and the dihedral angle between the two unsubstituted pyrazolates decreases to 110.2(2)°, as was also observed for the complex [(η^5 -C₅Me₅)Rh]₂(μ -pz)₂(μ -Cl)]BF₄.²⁴

The most conspicuous feature of all three structures is the

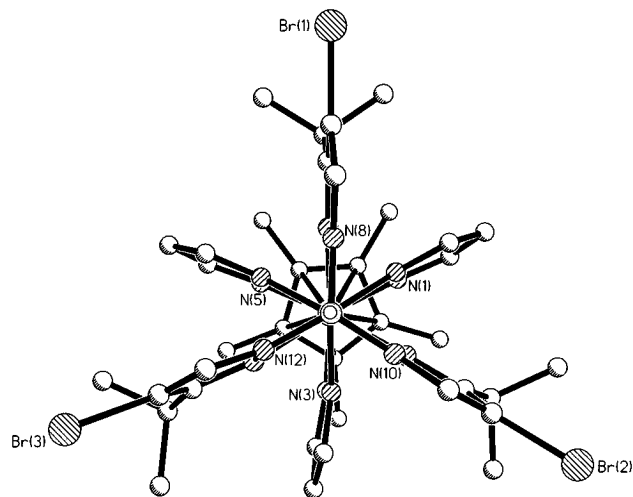


Figure 6. View of complex **13** along the B–Ni–Ir direction, showing the relative disposition of the two sets of pyrazolate ligands and the C₅Me₅ group.

slight trigonal distortion observed from the ideal octahedral coordination around the central metals—cobalt (**6**) or nickel (**12** and **13**)—arising from the different M'–N bond distances obtained for the 4-bromo-3-isopropylpyrazolate groups, significantly longer (0.144, 0.152, and 0.161 Å for **6**, **12**, and **13**, respectively) than those of the unsubstituted pyrazolates. A closer examination of the nonbonded distances for all the three complexes reveals contacts among the hydrogen atoms from the *i*-Pr group of the 4-bromo-3-isopropylpyrazolates and the nitrogen atoms of adjacent unsubstituted pyrazolate groups, clearly under the sum of van der Waals radii (shortest contacts: 2.51(1) Å for N(2)···H(23), 2.678(5) Å for N(4)···H(29), and 2.585(9) Å for N(2)···H(29), for **6**, **12**, and **13**, respectively). These data corroborate the idea that the coordination distortion, particularly the relative elongation of three M'–N distances, may result from the steric requirements of the isopropyl groups, repelling adjacent pyrazolate bridging ligands.³ The fact that complex **6** displays the least difference between the M'–N bonds of the two sets of bridging pyrazolates can be understood to be due to the presence of the less sterically demanding chloride bridge. Electronic factors should not, however, be discounted since the substituted pyrazolate groups bridging the M'–B centers might show donor qualities different from those of the “naked” pyrazolates bonded to the transition metals.

Acknowledgment. We thank the Dirección General de Investigación Científica y Técnica for financial support (Grants PB92/19 and PB94/1186), EC Human Capital and Mobility Programme (CT93-0347) (A.J.E.), CONICIT Venezuela (R.A.), and Prof. P. J. Alonso and Prof. F. Palacio for assistance with the EPR spectra and magnetic susceptibility measurements, respectively.

Supporting Information Available: Tables of hydrogen positional parameters, anisotropic displacement parameters, and complete bond distances and angles (32 pages). Ordering information is given on any current masthead page.

IC950896M

(29) Churchill, M. R.; Gold, K.; Maw, C. E., Jr. *Inorg. Chem.* **1970**, *9*, 1597.